

# Effect of Display Characteristics and Color Reproduction Method in Computerized Color Vision Test

Dan Zhang, Shining Ma, Yue Liu, Yongtian Wang, and Weitao Song; Beijing Institute of Technology; Beijing, China

## Abstract

A simulation was performed using simulated displays to examine how the results of the computerized color vision test are influenced by display characteristics, and color reproduction methods. In this work, the color difference between the background and the number in the test plates was employed to quantify the visibility of the target number in the computerized test. The results have indicated that for the color-appearance-based reproduction method, the impact of display characteristics on the target visibility is minimal except for the displays with extremely narrow bandwidth. While for the tristimulus-based reproduction method, it is necessary to consider display characteristics for the computerized color vision test.

## Introduction

The pseudoisochromatic plate (PIC) test has been widely used in occupational screening. It requires the tester to identify targets in the images and distinguishes individuals with abnormalities based on their recognition results. There are various types of PIC test, such as the Ishihara test commonly used for screening purposes, the AO-HRR test used for semi-quantitative evaluation, and the SPP II used for assessing acquired color vision impairment [1]. However, there are a few disadvantages of the paper-based pseudoisochromatic test, such as color fading, color inconsistency of printing, the possibility of cheating, etc. Recently, with the development of various display devices, computerized color vision test has gained increasing popularity which could provide pronounced convenience for color vision test. For example, computerized color vision test reduces the need to visit to hospitals, which can be conducted at home using devices such as computers and smartphones. However, there are differences between computerized and paper-based testing result. For example, the screening performance of the computerized color vision test (CCVT) is similar to other PIP tests, but the diagnostic performance differs [2]. The W-D15 and F-D15 tests do not exhibit perfect consistency [3]. The CCVT test shows a low level of agreement with the Ishihara test (with only 0.535 coefficient of consistency) [4]. The main reason for the differences is that the same images appear differently on different devices. This is primarily due to the characteristics of the displays and selected color reproduction methods. There are some studies on observer metamerism have shown that the chromaticity gamut and peak luminance level of display can affect the extent of observer metamerism (OMM) [5, 6]. When the peak luminance is doubled, the OMM increases by 7% to 8%, and OMM is related to the spectral bandwidth similarity between the displays.

Furthermore, the cross-media color reproduction method is another influential factor for the displayed colors. The color reproduction could take the XYZ tristimulus or color appearance as the profile connection space (PCS), corresponding to the colorimetry reproduction and color appearance reproduction, respectively. As indicated by many studies, the colorimetry reproduction works well for well-defined viewing conditions and fixed

output device [7]. Considering the effect of the viewing conditions and device medium, taking the appearance-based color space as PCS can better reproduce color appearance.

These factors are likely to influence the perception of color in computerized color vision tests, and several studies have already found discrepancies between computerized and paper-based color vision test results [8, 9, 10]. However, limited research has been conducted on the effects of display gamut and peak luminance on the performance of computerized color vision tests. Furthermore, there is a lack of standardized workflow for cross-media color reproduction in computerized color vision tests. This study aims to address these gaps by conducting a simulation-based analysis to assess the impact of display characteristics and color reproduction methods on the visibility of target numbers in computerized test plates.

## Procedures

### Test Plate Selection

Ishihara remains the most commonly used color vision test worldwide for detecting congenital red-green color vision abnormalities [1]. Numerous computerized versions have been developed based on the Ishihara test. In this study, the classification plate - No.22 plate of the latest 38<sup>th</sup> edition of Ishihara was selected as the test plate, as shown in Figure 1 (a). According to the Ishihara test instructions, the protanomalous color deficient observer (CDO) cannot see the number 2, while the deuteranomalous CDO cannot see the number 6. The color normal observer (CNO) can recognize the number 26 easily.

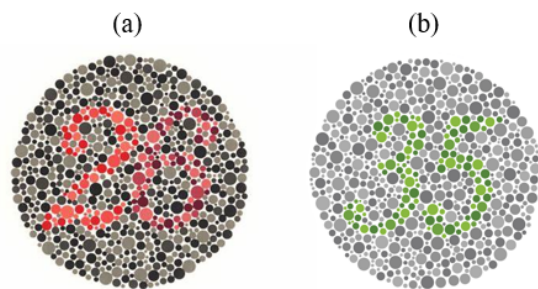


**Figure 1.** The test plates selected for the simulation-based analysis in this study. (a) Ishihara plate for the diagnosis of red-green color vision deficiency. (b) WCCVT's plate for testing blue color vision deficiency.

The Waggoner Computerized Color Vision test (WCCVT) is an advanced color vision testing suite developed by ophthalmic professionals, which includes a comprehensive range of color vision tests. As the Ishihara test focuses on the diagnosis of congenital red-green abnormality, we selected a specific test plate from the WCCVT for the diagnosis of tritanomalous CDO. It is worth noting that the WCCVT's Adult Diagnostic test is highly regarded and has been selected as one of three "precision" color vision tests available by the U.S.FAA [2]. The diagnostic test for WCCVT is capable of identifying tritanomalous CDO. Similar

to the Ishihara test, the WCCVT utilizes pseudoisochromatic test plates. In our study, we focused on a particular test plate with a greenish target number 35 and a greyish background, which is specifically designed for diagnosing tritanomalous CVD. Theoretically, individuals with tritanomalous CVD are unable to perceive the number 35, while those with normal color vision can easily recognize it.

The spectra of dots composing the background and target number in each test plate were measured by a Konica Minolta CS-2000 spectroradiometer with the measuring direction perpendicular to the target. The entire process has been carried out in a dark room. During the measurement, the Ishihara plate was illuminated by a D65 illumination with an illuminance of 300lx provided by a Datacolor Tru-Vue lighting booth. The test plate in WCCVT was displayed on a notebook (Thinkpad neo 14) with a sRGB chromaticity gamut and peak luminance of  $355cd/m^2$ .

### Color Matching Functions

The Asano model, which was initially developed for individual colorimetric observers, has demonstrated its effectiveness in representing the distribution of color matching functions (CMFs) within a population [11]. By adjusting the peak wavelength deviations [nm] from the average values for the L- and M-cone photopigments in the Asano model, the LMS cone fundamentals could be obtained for the protanomalous, deuteranomalous CDO, respectively. The range of peak wavelength shifts for L- and M-cone photopigments are  $[-20, 0]$ ,  $[0, 20]$  nm, respectively, with a 1 nm step. However, it is still uncertain if the inherited tritanomaly causes a large shift in the peak wavelength of the S-cone photopigment. Several studies on cone mosaics demonstrated an abnormal topographic distribution of S-cones for some tritanopes [12]. When simulating the cone fundamentals of tritanomalous CDO, we assumed that the peak wavelength of the S-cone photopigment absorbance curve shifted to that of the M-cone, with a shift range of  $[0, 100]$  nm in the Asano model.

The Yaguchi model was adopted to simulate the cone fundamentals for three types of anomalous trichromats where the spectral quantal absorption of the L-, M- or S- photopigments should shift along the wavenumber from the normal spectral absorption [13], as expressed in Equation 1. Furthermore, the simulated LMS cone fundamentals were normalized to ensure that equal-energy white appears white for all the observers [13], as illustrated in Equation 2:

$$\log A'_j(v) = \log A_j(v \pm \Delta v) \quad (1)$$

$$\begin{aligned} \bar{l}'(\lambda)_{new} &= \frac{L_{EEW}}{L'_{EEW}} \bar{l}(\lambda)_{new} \\ \bar{m}'(\lambda)_{new} &= \frac{M_{EEW}}{M'_{EEW}} \bar{m}(\lambda)_{new} \\ \bar{s}'(\lambda)_{new} &= \frac{S_{EEW}}{S'_{EEW}} \bar{s}(\lambda)_{new} \end{aligned} \quad (2)$$

where  $L_{EEW}$ ,  $M_{EEW}$  and  $S_{EEW}$  are the tristimulus values of equal-energy white for the CIE 2006 2° standard observer;  $L'_{EEW}$ ,  $M'_{EEW}$  and  $S'_{EEW}$  are those for simulated anomalous trichromats.  $\bar{l}'(\lambda)$ ,  $\bar{m}'(\lambda)$  and  $\bar{s}'(\lambda)$  are the simulated cone fundamentals for 2° field of view.  $\bar{l}(\lambda)_{new}$ ,  $\bar{m}(\lambda)_{new}$  and  $\bar{s}(\lambda)_{new}$  are the corrected cone fundamentals.

Then a total 120, 000 sets of LMSs were generated for 2° field of view, with observers aged 20-60 years, to ensure a large enough number of observers to provide a representative sample of individuals with various types and degrees of color vision abnormalities, as shown in Figure 2. Finally, the LMSs values were

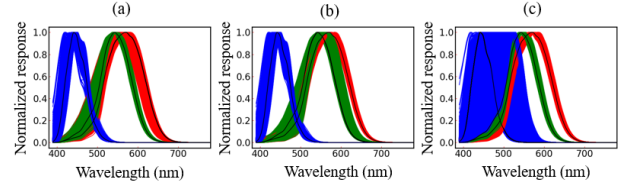


**Figure 2.** Simulated individual LMS cone fundamentals with different types and degrees of color vision abnormalities. The black solid lines represent the CIE 2006 2° standard observer. (a) The protanomalous CDO with a peak wavelength shift of the L-cone photopigment. (b) The deuteranomalous CDO with a peak wavelength shift of the M-cone photopigment. (c) The tritanomalous CDO with a peak wavelength shift of the S-cone photopigment.

converted to CMFs using the LMS-to-CMF conversion matrix provided by the CIE standard [14].

### Characteristics of the Display

Regarding the characteristics of the display, two parameters were primarily considered including the chromaticity gamut and the peak luminance. Three widely used chromaticity gamut standards, namely Rec.709, DCI.P3, and Rec.2020, were selected, as presented in Figure 3. As for the peak luminance, four levels were chosen: 200, 400, 600, 800, and  $1000cd/m^2$ . The white point for all three chromaticity gamuts was consistently assumed to be D65,  $(x,y)=(0.3127,0.3290)$ , according to the international HDR standard [15].

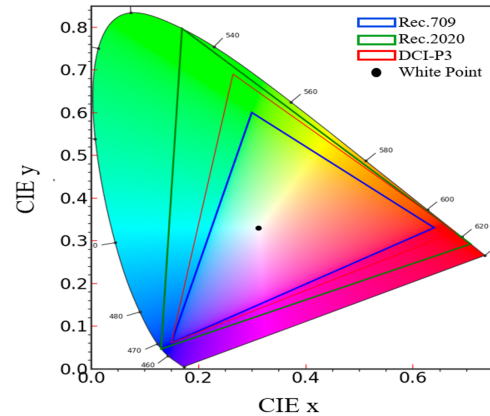


**Figure 3.** Three selected chromaticity gamuts for simulation-based analysis including Rec.709, DCI.P3, and Rec.2020 in the CIE 2006 2° x-y chromaticity diagram. The black point in the center represents the D65 white point.

The next step is to establish the spectra of three primaries (Red, Green, Blue) for simulated displays varying in chromaticity gamut and peak luminance. As suggested by Park et al. [5], the spectrum of each primary can be represented by a Gaussian function as given below:

$$S_M(\lambda, \mu, \sigma) = \frac{1}{\mu\sqrt{2\pi}} e^{-\frac{1}{2}\left(\frac{\lambda-\mu}{\sigma}\right)^2} \quad (3)$$

where M indicates a primary of a simulated display which can be Red (R), Green (G), or Blue (B);  $\lambda$  is the wavelength range (from 380 nm to 780 nm); parameter  $\mu$  and  $\sigma$  correspond to the peak wavelength and bandwidth of a primary which determine the chromaticity coordinates of a certain primary. The parameters  $\mu$  and  $\sigma$  of each channel were optimized to match the chromaticity coordinates of the corresponding chromaticity gamut.

The procedures for optimizing these parameters are explained in the following steps.

Firstly, to reduce the calculation cost,  $\mu$  and  $\sigma$  need to be discretized within a certain range. The parameter  $\mu$  has a range of [600, 630], [520, 560], [460, 480] nm for the red, green, and blue primary, respectively, with a step of 0.1 nm. The range of  $\sigma$  is limited to [0.1, 50] nm, with a step of 0.1 nm. Secondly, the simulated display does not provide XYZs tristimulus values but only  $x-y$  coordinates and peak luminance. To facilitate subsequent scaling calculations, it is assumed that each primary has the same fixed luminance value, denote as peak luminance  $L$ . The selection rules for  $\mu$  and  $\sigma$  are similar to Park's rules [5], where the combination that maximizes  $\sigma$  under the decision rule is chosen. The value of  $\mu$  and  $\sigma$  were optimized to minimize the  $DEu'_Fv'_F$  color difference (the Euclidean distance in CIE 1976  $u'_Fv'_F$  color space.) between the simulated and theoretical primary. According to the decision rule, the  $DEu'_Fv'_F$  should be less than 0.003. Additionally, if the decision rule cannot be met, for example, the red primary for Rec.709 and DCI.P3, the correction can be explained as given below:

$$\begin{bmatrix} X_M \\ Y_M \\ Z_M \end{bmatrix} = 683 \cdot C_{std} \cdot S_M \quad (4)$$

$$\begin{bmatrix} k_R \\ k_G \\ k_B \end{bmatrix} = \begin{bmatrix} X_R & X_G & X_B \\ Y_R & Y_G & Y_B \\ Z_R & Z_G & Z_B \end{bmatrix}^{-1} \cdot \begin{bmatrix} x \cdot \frac{L}{y} \\ L \\ (1-x-y) \cdot \frac{L}{y} \end{bmatrix} \quad (5)$$

$$S_{M,primary} = k_R \cdot S_R + k_G \cdot S_G + k_B \cdot S_B \quad (6)$$

where  $C_{std}$  indicate the CIE 2006 2° CMFs;  $S_M$  is the simulated spectrum of primary M, as calculated by Equation 3;  $X_M, Y_M, Z_M$  represent the XYZ tristimulus values of the simulated spectra  $S_M$ . And  $M$  can be Red (R), Green (G), or Blue (B) primary;  $x, y$  is the theoretical chromaticity coordinate of primary M in the standardized chromaticity gamut;  $L$  is the peak luminance of the display;  $k_R, k_G, k_B$  is the ratio of red, green, and blue required to form a fixed primary spectrum, respectively. Using the  $k_R, k_G, k_B$  values obtained from Equation 5, the corrected spectrum of primary M -  $S_{M,primary}$  can be calculated to meet the decision rule.

Thirdly, further adjustments are needed to ensure that the white point and the peak luminance meet the requirement. The chromaticity coordinates of the display's white point should be consistent with those of D65, so the luminance ratio of the three primaries can be derived from Equation 7. Then the spectra of three primaries are scaled using the luminance ratio to fit the peak luminance and white point requirements, see Equation 8.

$$\begin{bmatrix} n_R \\ n_G \\ n_B \end{bmatrix} = \begin{bmatrix} X_{R,primary} & X_{G,primary} & X_{B,primary} \\ Y_{R,primary} & Y_{G,primary} & Y_{B,primary} \\ Z_{R,primary} & Z_{G,primary} & Z_{B,primary} \end{bmatrix}^{-1} \cdot \begin{bmatrix} x_{D65} \cdot \frac{L}{y_{D65}} \\ L \\ (1-x_{D65}-y_{D65}) \cdot \frac{L}{0.3290} \end{bmatrix} \quad (7)$$

$$\begin{aligned} S'_R &= n_R \cdot S_{R,primary} \\ S'_G &= n_G \cdot S_{G,primary} \\ S'_B &= n_B \cdot S_{B,primary} \end{aligned} \quad (8)$$

where  $X_{M,primary}, Y_{M,primary}, Z_{M,primary}$  ( $M$  can be Red (R), Green (G) and Blue (B)) mean the tristimulus values of a primary calculated by  $S_{M,primary}$  derived from Equation 4;  $L$  is the

same as that in Equation 5;  $n_R, n_G, n_B$  are the scaling factors for the red, green and blue primary;  $S_{M,primary}$  is same as that in Equation 6;  $S'_M$  is the final spectrum of the primary M in the simulated display. Figure 4 shows the optimized spectra of three

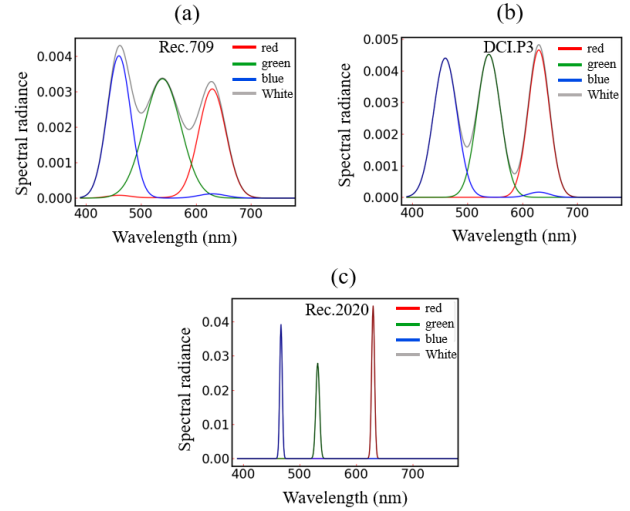


**Figure 4.** Spectra of simulated displays. It should be noted that all spectra have been scaled to represent displays with a peak luminance of  $200 \text{ cd/m}^2$ . (a) is the spectra of Rec.709. (b) is the spectra of DCI.P3. (c) is the spectra of Rec.2020.

**Table 1:**  $DEu'_Fv'_F$  color difference between the simulated and theoretical chromaticity of each primary

	Red	Green	Blue
Rec.709	5.55 e-17	1.21 e-4	8.77 e-17
DCI.P3	3.18 e-4	7.12 e-12	6.32 e-17
Rec.2020	1.20 e-3	3.28 e-4	7.55 e-4

simulated displays corresponding to three chromaticity gamuts. The optimization results successfully meet the requirements in terms of chromaticity gamut, white point coordinates, and peak luminance. Table 1 shows the  $DEu'_Fv'_F$  color difference between the simulated and theoretical chromaticity of each primary. As expected, the spectrum bandwidth of each primary becomes narrower as the chromaticity gamut expands.

## Methods of Color Reproduction

As computerized color vision tests are always conducted with personal computers or smartphones with various display characteristics, the method of cross-media color reproduction could greatly influence the color appearance displayed on the screen. The choice of PCS is a crucial consideration for color reproduction.

The first approach is to use CIE XYZ tristimulus values as the PCS in the color management workflow, known as colorimetry-based color reproduction [16]. The XYZ tristimulus values of the target dots in the selected test plates can be calculated from their measured spectra using CIE 2006 2° CMFs. To reproduce the colors with the same XYZ tristimulus values on the display, the ratios of the three primaries for each simulated display were calculated using Equation 9. Subsequently, the spectra of the reproduced colors on the simulated display can be estimated using the optimized spectrum of each primary (see

Figure 4).

$$\begin{aligned} \begin{bmatrix} P_R \\ P_G \\ P_B \end{bmatrix} &= [683 \cdot C_{std} \cdot [S'_R \quad S'_G \quad S'_B]]^{-1} \cdot \begin{bmatrix} X_{ref} \\ Y_{ref} \\ Z_{ref} \end{bmatrix} \\ &= [683 \cdot C_{std} \cdot [S'_R \quad S'_G \quad S'_B]]^{-1} \cdot 683 \cdot C_{std} \cdot S_{ref,color} \end{aligned} \quad (9)$$

$$S_{display,color} = P_R \cdot S'_R + P_G \cdot S'_G + P_B \cdot S'_B \quad (10)$$

where  $S_{ref,color}$  represents the measured spectra of the paper-based test plate;  $X_{ref}$ ,  $Y_{ref}$ ,  $Z_{ref}$  represent the tristimulus values of the  $S_{ref,color}$ ;  $S'_M$  ( $M$  can be R, G, and B) is same as that in Equation 8; the  $p_R$ ,  $p_G$ ,  $p_B$  is the primary ratio required to reproduce the color on the display.  $S_{display,color}$  is the spectra of color displayed in the simulated display.

Human color perception is not solely determined by XYZ tristimulus values but also influenced by various color appearance phenomena such as chromatic adaptation, Hunt effect, simultaneous contrast, etc. [17]. Color appearance models were proposed to build the bridge between colorimetry and color appearance attributes into account in color reproduction. Regarding the color appearance reproduction, CAM16-UCS was considered as PCS even though it was originally developed for reflective stimuli [16].

After the XYZ values of target colors were obtained from measured spectra, they were converted into  $J'a'b'$  coordinates in CAM16-UCS [18]. To reproduce the color appearance with consistent  $J'a'b'$  coordinates on the display, the  $J'a'b'$  coordinates were converted back into XYZ values using the inverse CAM16 model. Then the ratio of three primaries could be obtained, which subsequently enables deriving the spectra of the reproduced target colors on the simulated display.

The process for color reproduction based on the CAM16-UCS is shown through Equation 11 to 12.

$$\begin{aligned} &f_{cam16}(XYZ_{ref}, XYZ_{white,ref}, Y_{b,ref}) \\ &= [J'_{ref} \quad a'_{ref} \quad b'_{ref}]^T \quad (11) \\ &= f_{cam16}^{-1}(XYZ_{dispay}, XYZ_{white,dispay}, Y_{b,dispay}) \\ &\begin{bmatrix} P_R \\ P_G \\ P_B \end{bmatrix} = [683 \cdot C_{std} \cdot [S'_R \quad S'_G \quad S'_B]]^{-1} \cdot \begin{bmatrix} X_{dispay} \\ Y_{dispay} \\ Z_{dispay} \end{bmatrix} \quad (12) \end{aligned}$$

where  $f_{cam16}$  is the conversion formulas from XYZ to  $J'a'b'$  provided by the CAM16 model [18];  $f_{cam16}^{-1}$  is the inverse transformation from  $J'a'b'$  to XYZ;  $X_{display}$ ,  $Y_{display}$ ,  $Z_{display}$  are the tristimulus value of the color on displays;  $XYZ_{white,ref}$  and  $XYZ_{white,dispay}$  are the tristimulus value of the reference white of paper-based test and selected display, respectively;  $J'_{ref}$ ,  $a'_{ref}$ ,  $b'_{ref}$  are the  $J'a'b'$  values of the paper-based color;  $Y_{b,ref}$ ,  $Y_{b,dispay}$  are the background brightness of paper-based test and display, respectively;  $p_R$ ,  $p_G$ ,  $p_B$  are the primary ratio required to reproduce the color on the display. Through Equation 10, the spectra  $S_{display,color}$  reproduced on the simulated display can be calculated.

## Result & Discussion

The effects of chromaticity gamut and peak luminance on the visibility of the target number for three types of CDO were investigated using two different color reproduction methods. The simulations conducted a comparative analysis, which will be discussed in the following sections.

## Effect of Chromaticity Gamut

For individual observer, the spectra of all the unique dots composing the target number and background in the test plate (paper-based plate or computerized plate on a certain display) were used to calculate the LMS tristimulus using the cone fundamentals simulated by Asano model. Then the LMS tristimulus was converted to the XYZ tristimulus using the transformation function as defined by CIE [14]. Afterwards, the XYZ tristimulus of the target and background were calculated as the average tristimulus of the unique dots composing the number or background, respectively. By converting XYZ tristimulus into  $J'a'b'$  coordinates in CAM16-UCS, the color difference between the target number and background was computed, denoted as  $\Delta E_{Jab}$ .

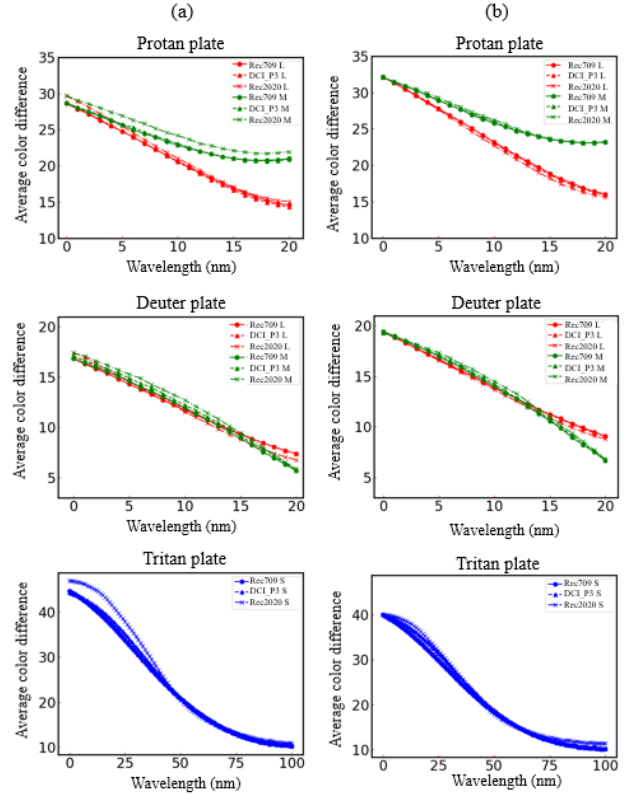


**Figure 5.** Effect of chromaticity gamut on the average color difference between the target number and background. In each subfigure, three line types correspond to three different chromaticity gamuts. (a) the simulation result using the colorimetry-based color reproduction method. (b) the simulation result using the color appearance reproduction method.

For each test plate, the color difference between the target number and background is a quantification metric to assess the visibility of the number. A larger color difference  $\Delta E_{Jab}$  indicates a higher likelihood of recognizing the target number. The severity of color vision abnormalities is represented by the peak wavelength shift of each photopigment, where a larger shift corresponds to a higher degree of color vision deficiency. Figure 5 presents the color difference  $\Delta E_{Jab}$  averaged over all the simulated observers against the peak wavelength shift for three chromaticity gamuts and three types of CDO. Six subfigures correspond to three test plates and two reproduction methods. The 'Protan plate' and 'Deuter plate' refer to the numbers '2' and '6' in the Ishihara test, used to test protanomalous and deuteranomalous color deficiencies, respectively. The 'Tritan plate' represents the test plate selected from WCCVT specific to tritanomalous color deficiency, as shown in Figure 1 (b). The three rows from

top to bottom represent the results for the 'Protan plate', 'Deuter plate', 'Tritan plate', respectively. The two columns correspond to two color reproduction methods with the XYZ tristimulus and CAM16-UCS coordinates as PCS. The color difference  $\Delta E_{Jab}$  decreases as the peak wavelength shift increases, indicating that the visibility of the target number decreases with the degree of color vision abnormalities, particularly when the type of color deficiency aligns with the test plate. Notably, the peak luminance of the display was maintained at  $200\text{cd}/\text{m}^2$  during the simulation of different chromaticity gamuts.

When color reproduction was performed based on the XYZ space, the expansion of the chromaticity gamut had a maximum impact of 14.48%, observed for the tritanomalous CDO when viewing the 'Tritan plate'. Figure 5 (a) illustrates that for the 'Protan plate' and 'Deuter plate', the influence of the chromaticity gamut gradually decreases as the degree of red-green color abnormality increases. For instance, when the peak wavelength of the L-cone in an individual observer shifts by more than 8 nm, the results obtained with Rec.709 and DCI.P3 chromaticity gamuts nearly overlap, and the difference between Rec.2020 and Rec.709 chromaticity gamuts is less than 6.65%. However, for the 'Tritan plate', the impact of the chromaticity gamut on the visibility of the target number becomes more pronounced with the higher degree of tritanomalous abnormality. In most cases, the average color difference between the target and background increases as the chromaticity gamut expands, particularly for the tritanomalous color deficiency when viewing the 'Tritan plate'. It implies that the target number reproduced on a narrow-band display (Rec.2020) can be more easily recognized than on displays with sRGB or DCI.P3 chromaticity gamut. Specifically, the difference in target number visibility between Rec.2020 and DCI.P3 chromaticity gamut is substantially larger than that between sRGB and DCI.P3. In summary, the effectiveness of computerized pseudoisochromatic color vision tests could be influenced by the chromaticity gamut of the display being used, especially when evaluating tritanomalous color deficiency using the 'Tritan plate'.

When color reproduction is performed using CAM16-UCS as the PCS, the influence of the chromaticity gamut on the color difference between the target and background is relatively small. In comparison to Figure 5 (a), Figure 5 (b) demonstrates a higher consistency among the three chromaticity gamuts, with a maximum chromaticity gamut influence of 6.37%. However, it is important to note that the chromaticity gamut has a significant impact on the diagnosis of tritanomalous color vision deficiency. The expansion of the chromaticity gamut results in a higher color difference between the target and background, and this trend becomes more pronounced as the tritanomalous abnormality increases.

Hence, the analysis conducted above indicates that the influence of the chromaticity gamut on the average color difference between the target number and background is dependent on the color reproduction method employed. To summarize, employing CAM16-UCS as the PCS in cross-media color reproduction can effectively mitigate the impact of the chromaticity gamut on the visibility of the target number in the test plate. However, this method yields a higher overall color difference between the target and background compared to colorimetry-based color reproduction, thereby enhancing the ease of observing the numbers by testers under the same experimental conditions. It is worth noting that for a chromaticity gamut with an extremely narrow bandwidth, such as Rec2020, the peak wavelength of the color gamut may also affect the results.

## Effect of Peak Luminance Level

Similar to the chromaticity gamut, the impact of display peak luminance on the effectiveness of computerized color vision test is also related to the color reproduction method. Figure 6 illustrates the relationship between the average target-background color difference and the peak luminance of the employed display for different degrees of color vision deficiency with varying peak wavelength shifts of the corresponding cone. As shown in Figure 6 (a), it is evident that the peak luminance of the display significantly affects the color difference when using the colorimetry-based color reproduction method. The color difference decreases as the peak wavelength increases, and this trend remains consistent across different chromaticity gamuts. For the sake of clarity, only the simulation results for Rec.709 have been presented in Figure 6. These results indicate that increasing the peak luminance of the display can decrease the visibility of the target number in the computerized color vision test. Furthermore, the effect of peak luminance on the color difference gradually diminishes as the values increase. For instance, the target-background color difference perceived by a CNO changes by 7.02% when the peak luminance increases from  $200\text{cd}/\text{m}^2$  to  $400\text{cd}/\text{m}^2$ , whereas it only changes by 2.35% when peak luminance increases from  $800\text{cd}/\text{m}^2$  to  $1000\text{cd}/\text{m}^2$ .

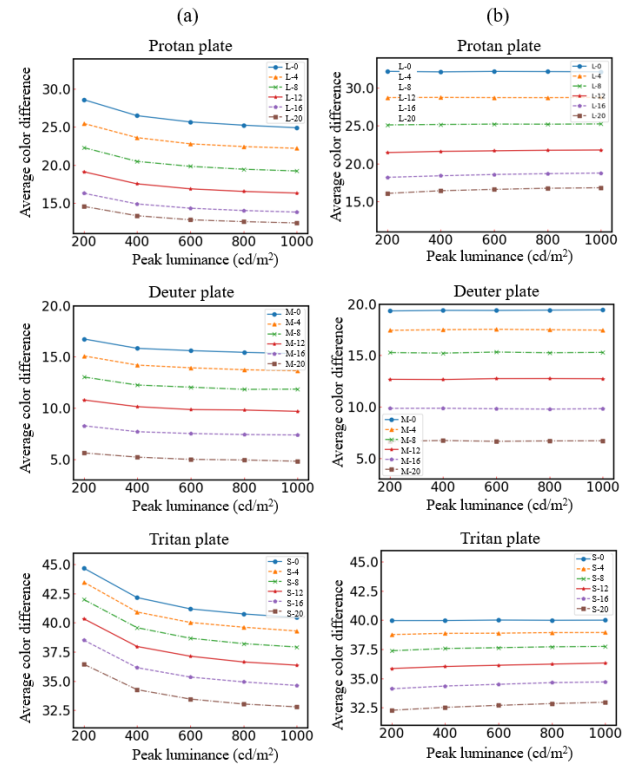


**Figure 6.** Effect of peak luminance on number visibility. Note that different colors indicate different degrees of color vision deficiency. (a) the simulation result using the colorimetry-based color reproduction method. (b) the simulation result using the color appearance reproduction method.

The negative relationship between the display peak wavelength and color difference follows theoretical expectations. With the increasing luminance of the reference white, the lightness of reproduced color patch decreases with the peak luminance, leading to a lower colorfulness of the target dots in the test plate. Then the perceived color difference between the target number and the background becomes smaller.

When employing CAM16-UCS for color reproduction, the

influence of peak luminance on the color difference is significantly diminished compared to the colorimetry-based method. In the case of the colorimetry-based method, increasing the peak luminance from  $200\text{cd}/\text{m}^2$  to  $1000\text{cd}/\text{m}^2$  results in a maximum change in color difference of 15.58%, as shown in Figure 6 (a). However, when utilizing the CAM16-UCS reproduction method, the target-background color difference only varies by 1.39%, with a high level of consistency among the curves at different peak luminance levels, reaching 99%. This outcome is consistent with our expectations, as the CAM16-UCS method considers the influence of the reference white on the perceived color appearance. Obviously, using CAM16-UCS as PCS for color reproduction can greatly reduce the impact of peak brightness on the effectiveness of diagnosis. If the colorimetry-based method was adopted for color reproduction, it is necessary to restrict the peak wavelength range of the displays used for the test.

## Conclusion

This paper extensively investigated the effect of display characteristics (chromaticity gamut, peak luminance), and color reproduction method on the effectiveness of the computerized color vision test through simulations. The simulations involved the generation of a total of 120,000 individual color matching functions using the model proposed by Asano, encompassing various types and severity levels of color vision deficiencies. To represent commonly used chromaticity gamuts, the spectra of three primaries were generated for displays with Rec.709, DCI.03, and Rec.2020 chromaticity gamuts, respectively. The peak luminance levels of these displays were set at 200, 400, 600, 800,  $1000\text{cd}/\text{m}^2$ . Test plates commonly used for the diagnosis of three types of CDO were carefully selected, and accurately reproduced on the simulated displays.

The simulation results indicate that the color reproduction method has a significant impact on the computerized color vision test. Employing CAM16-UCS for color reproduction can effectively mitigate the impact of the chromaticity gamut on the visibility of the target number in the test plate, with a maximum impact of only 6.37%. However, this method will result in enhancing the ease of observing the numbers by testers under the same experimental conditions. Additionally, the results for different peak luminance levels are highly consistent, indicating that the color appearance reproduction method can greatly reduce the impact of peak luminance on diagnostic effectiveness. When color reproduction was performed based on the XYZ space, the effectiveness of the computerized color vision test may be affected by the chromaticity gamut. The target numbers reproduced on narrow-band displays are easier to recognize. Furthermore, the impact of peak luminance on target-background color difference is quite large, reaching up to 15.58%, which should not be overlooked.

Therefore, when developing the computerized color vision test, it is recommended to use an appearance-based color space as PCS for cross-media. If color reproduction is performed on the XYZ space, it is necessary to impose restrictions on the peak luminance and chromaticity gamut of the selected display.

## References

- [1] Stephen J Dain. Clinical colour vision tests. *Clinical and Experimental Optometry*, 87(4-5):276–293, 2004.
- [2] Jason S Ng, Eriko Self, John E Vanston, Andrew L Nguyen, and Michael A Crognale. Evaluation of the waggoner computerized color vision test. *Optometry and Vision Science*, 92(4):480–486, 2015.

- [3] Ali Almustanyir, Reema Alduhayan, Mosaad Alhassan, Kholoud Bokhary, and Balsam Alabdulkader. Evaluation of the waggoner computerized d15 color vision test using an ipad device. *JOSA A*, 38(11):1647–1655, 2021.
- [4] Nir Sorkin, Amir Rosenblatt, Eyal Cohen, Oded Ohana, Chaim Stolovitch, and Gad Dotan. Comparison of isihara booklet with color vision smartphone applications. *Optometry and Vision Science*, 93(7):667–672, 2016.
- [5] Yongmin Park and Michael J Murdoch. Efficiently evaluating the effect of color gamut and spectral bandwidth on observer metamerism in high dynamic range displays. *Journal of the Society for Information Display*, 29(9):704–722, 2021.
- [6] Yongmin Park and Michael Murdoch. Effect of color gamut and luminance on observer metamerism in hdr displays. 2020.
- [7] Yiqian Li, Siyuan Chen, Minchen Wei, and Xiandou Zhang. Consideration of degree of chromatic adaptation for reproducing illuminated scenes. *Color Research & Application*, 47(3):605–614, 2022.
- [8] MP Simunovic. Colour vision deficiency. *Eye*, 24(5):747–755, 2010.
- [9] Stephen J Dain and Ali AlMerdef. Colorimetric evaluation of iphone apps for colour vision tests based on the isihara test. *Clinical and Experimental Optometry*, 99(3):264–273, 2016.
- [10] Jayasree Seshadri, Jerry Christensen, Vasudevan Lakshminarayanan, and Carl J Bassi. Evaluation of the new web-based “colour assessment and diagnosis” test. *Optometry and vision science*, 82(10):882–885, 2005.
- [11] Yuta Asano, Mark D Fairchild, and Laurent Blondé. Individual colorimetric observer model. *PloS one*, 11(2):e0145671, 2016.
- [12] Rigmor C Baraas, Joseph Carroll, Karen L Gunther, Mina Chung, David R Williams, David H Foster, and Maureen Neitz. Adaptive optics retinal imaging reveals s-cone dystrophy in tritan color-vision deficiency. *JOSA A*, 24(5):1438–1447, 2007.
- [13] Hirohisa Yaguchi, Junyan Luo, Miharuru Kato, and Yoko Mizokami. Computerized simulation of color appearance for anomalous trichromats using the multispectral image. *JOSA A*, 35(4):B278–B286, 2018.
- [14] Francoise Vienot. Fundamental chromaticity diagram with physiologically significant axes. In *9th Congress of the International Colour Association*, volume 4421, pages 565–570. SPIE, 2002.
- [15] BT ITU-R. Image parameter values for high dynamic range television for use in production and international programme exchange. *Image parameter values for high dynamic range television for use in production and international programme exchange*, 2016.
- [16] Shining Ma, Kees Teunissen, and Kevin AG Smet. Predictive performance of the standard and the modified von kries chromatic adaptation transforms. *Optics Express*, 30(7):11872–11891, 2022.
- [17] M Ronnier Luo and MR Pointer. Cie colour appearance models: A current perspective. *Lighting Research & Technology*, 50(1):129–140, 2018.
- [18] Changjun Li, Zhiqiang Li, Zhifeng Wang, Yang Xu, Ming Ronnier Luo, Guihua Cui, Manuel Melgosa, Michael H Brill, and Michael Pointer. Comprehensive color solutions: Cam16, cat16, and cam16-ucs. *Color Research & Application*, 42(6):703–718, 2017.

## Author Biography

Dan Zhang is a PhD student at the Beijing Institute of Technology. She received her bachelor degrees from Beijing Institute of Technology.